

FULL PAPER

Synthesis and characterization of Ni(II) complexes bearing of 2-(1*H*-benzimidazol-2-yl)-phenol derivatives as highly active catalysts for ethylene oligomerization

Marzieh Haghverdi¹ | Azadeh Tadjarodi¹  | Naeimeh Bahri-Laleh² | Mehdi Nekoomanesh-Haghighi²

¹Research Laboratory of Inorganic Materials Synthesis, Department of Chemistry, Iran University of Science and Technology, Tehran, Iran

²Polymerization Engineering Department, Iran Polymer and Petrochemical Institute (IPPI), Tehran, Iran

Correspondence

Azadeh Tadjarodi, Research Laboratory of Inorganic Materials Synthesis, Department of Chemistry, Iran University of Science and Technology, Tehran, Iran. Email: tadjarodi@iust.ac.ir

Funding information

Iran University of Science and Technology, Iran Polymer and Petrochemical Institute and Petrochemical Research & Technology Company

Novel Ni(II) complexes of 2-(1*H*-benzimidazol-2-yl)-phenol derivatives (HL_{*x*}; *x* = 1–5; **C1**–**C5**) have been synthesized and characterized. In the mononuclear complexes, the ligands were coordinated as bidentate, via one imine nitrogen and the phenolate oxygen atoms. The structures of the compounds were confirmed on the basis of FT-IR, UV–Vis, ¹H-, ¹³C–NMR, inductively coupled plasma and elemental analyses (C, H and N). The purity of these compounds was ascertained by melting point (m.p.) and thin-layer chromatography. The geometry optimization and vibrational frequency calculations of the compounds were performed using Gaussian 09 program with B3LYP/TZVP level of theory. All Ni(II) complexes were activated with diethylaluminum chloride (Et₂AlCl), so that **C2** showed the highest activity [6600 kg mol^{−1} (Ni) h^{−1}], where the ligand contains a chlorine substituent. Oligomers obtained from the complexes consist mainly of dimer and trimer, and also exhibit high selectivity for linear 1-butene and 1-hexene. Both the steric and electronic effects of coordinative ligands affect the catalytic activity and the properties of the catalytic products.

KEYWORDS

benzimidazolylphenols, density functional theory calculations, ethylene oligomerization, nickel (II) complexes

1 | INTRODUCTION

The oligomerization of ethylene is the major industrial process to produce linear α -olefins. These linear α -olefins are extensively used in the preparation of detergents, plasticizers and synthetic lubricants. They are also known as comonomers to produce linear low-density polyethylene.^[1]

Research on late transition-metal complexes as catalysts for ethylene oligomerization and polymerization has attracted considerable attention in both academic and industrial circles due to their high activity and selectivity, as well as their lower oxophilicity and tolerance of functional groups.^[2]

Favored application of late transition-metal complexes as catalysts for ethylene oligomerization was first achieved industrially through employing nickel complexes in the shell higher olefin process.^[3] To extend the efficient catalytic systems, nickel complexes bearing bidentate ligands such as N[^]N, N[^]O and P[^]N have been extensively studied.^[4] Benzimidazolyl-phenol is a type of N[^]O ligand. The complexes with these ligands are important, because of high thermal stability, better catalytic performance, superior optical properties,^[5] as well as strong chelating agents. Benzimidazolyl-phenol and its derivatives can also coordinate as monodentate or multidentate via one imine nitrogen atom and a phenolate oxygen atom

to form M–N and M–O bonds. Besides, it can also act as a donor and (or) acceptor in hydrogen bond interactions.^[6] The synthesis of privileged chemicals through an economical and environmentally friendly method is always desirable. The reaction of substituted *o*-phenylenediamine with 2-hydroxy aromatic aldehydes is the common method to produce benzimidazolyl-phenol derivatives.^[7]

In order to improve catalytic activities of metal complexes and finely tune their products, the design of catalysts for ethylene oligomerization and polymerization is important. The useful way to modify ligands is by placing different substituents on the frame of ligands.^[8] In the case of benzimidazolyl-phenol ligands, it is very difficult to further modify the imidazole ring of benzimidazole, therefore the functionalization of benzimidazole will be fused with the benzene ring.

Here we report the synthesis and characterization of various 1*H*-benzimidazol-2-yl-phenol derivatives and their Ni(II) complexes. The optimized geometry and vibrational frequency calculations of the compounds were derived from theoretical calculations in B3LYP/TZVP level using Gaussian 09 program. The experimental results were in agreement with the theoretical calculations. Also, we reported the correlation among complex structures, catalytic activities and product properties. These complexes have been evaluated in the oligomerization of ethylene upon treatment with diethylaluminum chloride (Et₂AlCl).

2 | EXPERIMENTAL

2.1 | Materials and measurements

All manipulations of air- and moisture-sensitive compounds were performed under a nitrogen atmosphere using standard Schlenk techniques. Toluene was refluxed over sodium-benzophenone and distilled under nitrogen. All reagents (including Et₂AlCl) were purchased from Aldrich, Merck or Acros Chemicals. Elemental analysis was carried out on a Perkin Elmer model 2400 series 2 automatic carbon, hydrogen, nitrogen analyzer. The determination of metal percentage was performed using inductively coupled plasma (ICP; 3410ARL model). IR spectra were recorded on Shimadzu FT-IR 8400 spectrometer by using KBr disc in the range of 400–4000 cm⁻¹. UV spectra were obtained using a Shimadzu, UV-1700 spectrophotometer in dimethyl sulfoxide (DMSO) solution. NMR spectra (300 MHz for ¹H and 75 MHz for ¹³C) were recorded on a Bruker AVANCE-300 instrument in DMSO-d₆ using tetramethylsilane as internal standard. Gas chromatography (GC) analysis was performed using a Varian CP-3800 gas chromatograph equipped with a flame ionization detector and a 100 m (0.25 mm i.d., 0.5 μm film thickness) CP-Sil PONA CB. The yield of

oligomers was calculated by referencing to the mass of the solvent on the basis of the prerequisite that the mass of each fraction was approximately proportional to its integrated areas in the GC trace. Selectivity for linear 1-alkenes was defined as: amount of linear 1-alkenes of all fractions/total amount of oligomer products (as a percentage). Melting points were determined using an electro thermal melting point apparatus. The completion of reactions was monitored by thin-layer chromatography (TLC).

2.2 | Synthesis of the ligands

2.2.1 | 2-(1*H*-Benzimidazol-2-yl)-phenol (HL₁)

2-Hydroxybenzaldehyde (1.83 g, 15.0 mmol) and sodium metabisulfide (1.60 g, 8.5 mmol) were dissolved in 20 ml of ethanol and 20 ml water, respectively. The reaction mixture was stirred vigorously and more ethanol was added. The mixture was kept in a refrigerator for several hours. The mixture was filtered and sodium hydroxyl (2-hydroxyphenyl) methansulfonate salt obtained from the crude extract. This crude salt and 1,2-phenylenediamine (0.43 g, 4.0 mmol) in 10 ml of DMF were refluxed for 4 h at 130 °C in an oil bath. The completion of reaction was monitored by TLC. Then, the mixture was poured in an ice bath. After that the reaction was quenched by adding water, and 2-(1*H*-benzimidazole-2-yl) phenol filtered and recrystallized from ethanol.^[9] This method was selected because of simplicity, high yields and saving time. This intermediate compound (namely, bisulfite compound of the aldehyde) was utilized to catalyze the benzimidazole synthesis, as 1,2-phenylenediamines and aldehydes do not produce a cyclization reaction by themselves under mild conditions and possibly might lead to Schiff bases. 2-(1*H*-Benzimidazole-2-yl) phenol was used for the synthesis of the complexes. Brown creamy powder, yield: 71.43%. m.p.: 239–240 °C. ¹H-NMR (CDCl₃, 300 MHz): δ 6.96 (t, 1H, *J* = 7.35 Hz), 7.14 (d, 1H, *J* = 8.30 Hz), 7.32 (m, 2H), 7.58 (d, 2H, *J* = 12.72 Hz), 7.72 (s, 1H), 9.44 (s, 1H, N-H), 13.07 (s, 1H, O-H). ¹³C-NMR (CDCl₃, 75 MHz): 112.08, 118.16, 119.02, 123.34, 124.37, 132.04, 151.35, 158.98. IR (KBr disc, cm⁻¹): 3325, 3245, 3053, 2300, 1629, 1591, 1490, 1460, 1417, 1394, 1276, 1130, 838, 675. Anal. calcd for C₁₃H₁₀N₂O: C, 74.27, H, 4.79; N, 13.33. Found: C, 75.02; H, 4.32; N, 12.22%.

2.2.2 | 2-(5-Chloro-1*H*-benzimidazol-2-yl)-phenol (HL₂)

HL₂ was prepared by using the same procedure as the synthesis of HL₁, except that 4-chloro-*o*-phenylenediamine was used instead of 1,2-phenylenediamine. Dark brown

powder, yield: 60%. m.p.: 281–282 °C. $^1\text{H-NMR}$ (CDCl_3 , 300 MHz): δ 7.01 (m, 2H), 7.26 (d, 1H, $J = 8.37$ Hz), 7.37 (t, 1H, $J = 7.59$ Hz), 7.64 (s, 1H), 7.74 (s, 1H), 8.04 (d, 1H, $J = 7.7$ Hz), 12.76 (s, 1H, N-H), 13.26 (s, 1H, O-H). $^{13}\text{C-NMR}$ (CDCl_3 , 75 MHz): 112.52, 117.23, 117.50, 117.65, 119.27, 123.07, 126.59, 132.05, 152.85, 157.87. IR (KBr disc, cm^{-1}): 3328, 3014, 2310, 1633, 1583, 1488, 1465, 1421, 1382, 1282, 1134, 1058, 844, 705. Anal. calcd for $\text{C}_{13}\text{H}_9\text{N}_2\text{OCl}$: C, 63.81, H, 3.68; N, 11.45. Found: C, 62.11; H, 3.38; N, 10.98%.

2.2.3 | 2-(5-methyl-1H-benzimidazol-2-yl)-phenol (HL₃)

HL₃ was prepared by using the same procedure as the synthesis of HL₁, except that 4-methyl-o-phenylenediamine was used instead of 1,2-phenylenediamine. Cream brownish powder, yield: 50%. m.p.: 255–256 °C. $^1\text{H-NMR}$ (CDCl_3 , 300 MHz): δ 2.42 (s, 3H, CH_3), 7.01 (m, 2H), 7.08 (d, 1H, $J = 8.16$ Hz), 7.35 (t, 1H, $J = 7.26$ Hz), 7.43 (s, 1H), 7.53 (d, 1H, $J = 8.13$ Hz), 8.03 (d, 1H, $J = 7.71$ Hz), 13.14 (s, 2H, N-H, O-H). $^{13}\text{C-NMR}$ (CDCl_3 , 75 MHz): 21.29, 112.69, 117.15, 119.05, 124.29, 126.05, 131.54, 132.26, 151.40, 157.98. IR (KBr disc, cm^{-1}): 3236, 3082, 3028, 2914, 2858, 2212, 1735, 1637, 1596, 1488, 1456, 1419, 1390, 1261, 1130, 846, 680. Anal. calcd for $\text{C}_{14}\text{H}_{12}\text{N}_2\text{O}$: C, 74.98, H, 5.35; N, 12.49. Found: C, 73.98; H, 4.79; N, 12.15%.

2.2.4 | 2-(5,6-Dichloro-1H-benzimidazol-2-yl)-phenol (HL₄)

HL₄ was prepared by using the same procedure as the synthesis of HL₁, except that 4,5-dichlorobenzene-1,2-diamine was used instead of 1,2-phenylenediamine. Pink powder, yield: 50%. m.p.: 327–328 °C. $^1\text{H-NMR}$ (CDCl_3 , 300 MHz): δ 7.01 (m, 2H), 7.38 (t, 1H, $J = 7.48$ Hz), 7.87 (s, 2H), 8.05 (d, 1H, $J = 7.66$ Hz), 12.50 (s, 2H, N-H, O-H). $^{13}\text{C-NMR}$ (CDCl_3 , 75 MHz): 112.54, 116.08, 117.21, 119.36, 124.99, 127.00, 132.30, 133.53, 153.77, 157.71. IR (KBr disc, cm^{-1}): 3332, 3097, 2320, 1637, 1598, 1487, 1444, 1419, 1371, 1298, 1132, 1097, 864, 740. Anal. calcd for $\text{C}_{13}\text{H}_8\text{N}_2\text{OCl}_2$: C, 55.94, H, 2.89; N, 10.04. Found: C, 55.68; H, 2.94; N, 9.61%.

2.2.5 | 2-(5,6-dimethyl-1H-benzimidazol-2-yl)-phenol (HL₅)

HL₅ was prepared by using the same procedure as the synthesis of HL₁, except that 4,5-dimethylbenzene-1,2-diamine was used instead of 1,2-phenylenediamine. Cream powder, yield: 50%. m.p.: 297–298 °C. $^1\text{H-NMR}$ (CDCl_3 , 300 MHz): δ 2.32 (s, 6H, CH_3), 6.98 (m, 2H),

7.33 (t, 1H, $J = 7.56$ Hz), 7.40 (s, 2H), 8.00 (d, 1H, $J = 7.69$ Hz), 13.11 (s, 2H, N-H, O-H). $^{13}\text{C-NMR}$ (CDCl_3 , 75 MHz): 19.96, 112.79, 117.08, 118.96, 125.88, 131.31, 131.48, 150.83, 157.92. IR (KBr disc, cm^{-1}): 3257, 3124, 3049, 2970, 2858, 2241, 1637, 1589, 1488, 1461, 1417, 1384, 1257, 1130, 852, 675. Anal. calcd for $\text{C}_{15}\text{H}_{14}\text{N}_2\text{O}$: C, 75.63, H, 5.88; N, 11.76. Found: C, 74.29; H, 5.82; N, 11.42%.

The structure of the synthesized ligands is given in Scheme 1. Except for HL₄, these ligands had been synthesized before.^[9]

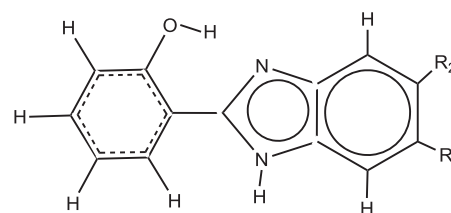
2.3 | Synthesis of the complexes C1–C5

2.3.1 | $\text{K}_2[\text{Ni}(\text{HL}_1)_2\text{Cl}_2] \cdot 2\text{H}_2\text{O}$ (C1)

A solution of HL₁ (0.106 g, 0.5 mmol) and KOH (0.028 g, 0.5 mmol) in methanol was added to a solution of $\text{NiCl}_2 \cdot 6\text{H}_2\text{O}$ (0.059 g, 0.25 mmol) in methanol. The color change took place immediately. The resulting solution was stirred for 24 h at room temperature. The completion of the reaction was monitored by TLC. The precipitation appeared in the resulting solution after a few days (by slow evaporation of the solvent). The resulting precipitation was separated by filtration, washed with diethyl ether and dried in vacuum. Olive powder, yield: 50%. IR (KBr disc, cm^{-1}): 3419 (N-H), 3058 (C-H), 1623 (C = N), 1527 (C = C), 1255 (C-O), 486 (Ni-O), 418 (Ni-N). Anal. calcd for $\text{C}_{26}\text{H}_{22}\text{N}_4\text{O}_4\text{K}_2\text{Cl}_2\text{Ni}$: C, 47.15, H, 3.32, N, 8.46, Ni, 8.86. Found: C, 48.00, H, 2.97, N, 7.60, Ni, 8.81%.

2.3.2 | $\text{K}_2[\text{Ni}(\text{HL}_2)_2\text{Cl}_2] \cdot 2\text{H}_2\text{O}$ (C2)

C2 was prepared in the same way as C1. Olive powder, yield: 70.87%. IR (KBr disc, cm^{-1}): 3433 (N-H), 3176 (C-H), 1623 (C = N), 1560 (C = C), 1253 (C-O), 480 (Ni-O), 418 (Ni-N). Anal. calcd for $\text{C}_{26}\text{H}_{20}\text{N}_4\text{O}_4\text{K}_2\text{Cl}_4\text{Ni}$: C, 42.69, H, 2.73, N, 7.66, Ni, 8.03. Found: C, 44.62, H, 2.18, N, 6.00, Ni, 7.70%.



HL₁: R₁=R₂=H

HL₂: R₁=Cl, R₂=H

HL₃: R₁=CH₃, R₂=H

HL₄: R₁=R₂=Cl

HL₅: R₁=R₂=CH₃

SCHEME 1 Structure of the synthesized ligands

2.3.3 | $K_2[Ni(HL_3)_2Cl_2]$ (C3)

C3 was prepared in the same way as **C1**. Olive powder, yield: 52.76%. IR (KBr disc, cm^{-1}): 3417 (N-H), 3180 (C-H), 1628 (C = N), 1562 (C = C), 1261 (C-O), 487 (Ni-O), 439 (Ni-N). Anal. calcd for $C_{28}H_{22}N_4O_2K_2Cl_2Ni$: C, 51.40, H, 3.36, N, 8.56, Ni, 8.97. Found: C, 49.64, H, 2.97, N, 8.30, Ni, 9.28%.

2.3.4 | $K_2[Ni(HL_4)_2Cl_2] \cdot 3H_2O$ (C4)

C4 was prepared in the same way as **C1**. Olive powder, yield: 46%. IR (KBr disc, cm^{-1}): 3419 (N-H), 3060 (C-H), 1625 (C = N), 1558 (C = C), 1255 (C-O), 451 (Ni-O), 439 (Ni-N). Anal. calcd for $C_{26}H_{18}N_4O_4K_2Cl_6Ni$: C, 38.15, H, 2.44, N, 6.84, Ni, 7.18. Found: C, 38.45, H, 1.70, N, 5.00, Ni, 8.76%.

2.3.5 | $[Ni(HL_5)_2]$ (C5)

C5 was prepared in the same way as **C1**. Mustard powder, yield: 40%. IR (KBr disc, cm^{-1}): 3404 (N-H), 3055 (C-H), 1635 (C = N), 1550 (C = C), 1247 (C-O), 476 (Ni-O), 430 (Ni-N). Anal. calcd for $C_{30}H_{26}N_4O_2Ni$: C, 67.58, H, 4.88, N, 10.51, Ni, 11.01. Found: C, 66.92, H, 4.69, N, 10.19, Ni, 12.73%.

2.4 | Computational details

Full geometry optimizations were carried out using the density functional theory (DFT) method at the B3LYP, the hybrid GGA functional theory of Becke-Lee, Parr and Yang,^[10,11] level for HL_{1-5} ligands and **C1–C5** complexes, because, as reported before, better agreement with the experimental results can be obtained with B3LYP and it is a commonly used functional in the molecular simulation of transition-metal catalytic systems.^[12–16] In all cases, the electronic configuration of the molecular systems was described with the triple- ζ basis set augmented with one-polarization functions of Ahlrichs and co-workers (TZVP keyword in Gaussian).^[17] All calculations were performed by the Gaussian 09 program.^[18] For all the computed complexes, except **C5**, the triplet was the electronic ground state and thus open shell calculations were performed. In the case of **C5**, the singlet was the ground state and closed shell calculations were employed.

The vibrational frequency calculations were also performed to ensure that the optimized geometries represent the local minima and that there are only positive Eigen values.^[19,20] The optimized geometry of compounds furnished the total energy. The energy values obtained by using the DFT calculations are: HL_1 (−686), HL_2 (−1146), HL_3 (−726), HL_4 (−1606), HL_5 (−765), whereas

C1 (−3801), **C2** (−4720), **C3** (−3879), **C4** (−5639) and **C5** (−3037). The energy values are in a.u. and indicate that the complexes have more stability compared with ligands.^[21]

2.5 | Procedure for ethylene oligomerization

Ethylene oligomerization was performed in a stainless-steel autoclave (1-l capacity) equipped with a gas ballast through a solenoid valve for continuous feeding of ethylene at constant pressure. First, 100 ml of toluene was transferred to the fully dried reactor under a nitrogen atmosphere. The required amount of Et_2AlCl was then injected into the reactor via a syringe. Next, toluene solution of catalytic precursor was added to the reactor under a nitrogen atmosphere. Over the reaction temperature, the reactor was sealed and pressurized to high ethylene pressure, and the ethylene pressure was maintained during feeding of ethylene. After stirring the reaction mixture for 30 min, the reaction was stopped by cooling the reactor before releasing the excess pressure and a small amount of the reaction solution was collected, which was then analyzed by GC to determine the composition and mass distribution of the oligomers obtained. The residual reaction solution was quenched with 5% hydrochloric acid ethanol to collect the polyethylene obtained; although polyethylene was not formed.

3 | RESULTS AND DISCUSSION

The analytical data and physical properties of the ligands and complexes were summarized in Table 1. The **C1** and **C2** complexes had the general composition of $K_2[Ni(HL_{1,2})_2Cl_2] \cdot 2H_2O$. Also, the general formulae for the **C3** and **C4** complexes were $K_2[Ni(HL_3)_2Cl_2]$ and $K_2[Ni(HL_4)_2Cl_2] \cdot 3H_2O$, respectively, and for **C5** was $[Ni(HL_5)_2]$. Six-coordinated octahedral structures have been assigned for the **C1–C4** complexes, while the **C5** complex has square-planar geometry. These results were confirmed by IR spectra, UV-Vis, ICP and elemental analysis (C, H and N). The melting points of the ligands HL_2 – HL_5 suggest that chloro and methyl substitutions on the benzimidazole moiety increase melting points with respect to HL_1 ligand.^[22] Many attempts have been made in obtaining single crystals of all complexes, but suitable crystals have not been found in order to determine the crystal structure of these compounds. Therefore, we decided to use DFT calculations in order to determine the molecular structures of complexes. The optimized structures, vibrational frequencies, stability of the ligands and complexes, as well as the various bond lengths and

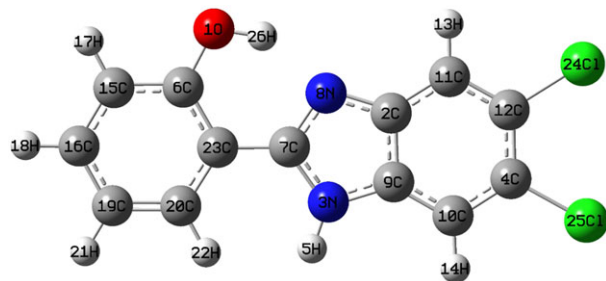
TABLE 1 The analytical data and physical properties of the ligands and complexes

Compound	Elemental analysis: found			(Calcd) % Ni	Yield %	m.p. °C	Color
	C	N	H				
HL ₁ C ₁₃ H ₁₀ N ₂ O	75.02 (74.27)	4.32 (4.79)	12.22 (13.33)	—	71.43	239–240	Brown creamy
HL ₂ C ₁₃ H ₉ N ₂ OCl	62.11 (63.81)	3.38 (3.68)	10.98 (11.45)	—	60	281–282	Dark brown
HL ₃ C ₁₄ H ₁₂ N ₂ O	73.98 (74.98)	4.79 (5.35)	12.15 (12.49)	—	50	255–256	Cream brownish
HL ₄ C ₁₃ H ₈ N ₂ OCl ₂	55.68 (55.94)	2.94 (2.89)	9.61 (10.04)	—	50	327–328	Pink
HL ₅ C ₁₅ H ₁₄ N ₂ O	74.29 (75.63)	5.82 (5.88)	11.42 (11.76)	—	50	297–298	Cream
K ₂ [Ni (HL ₁) ₂ Cl ₂]2H ₂ O C ₂₆ H ₂₂ N ₄ O ₄ K ₂ Cl ₂ Ni	48.00 (47.15)	2.97 (3.32)	7.60 (8.46)	8.81 (8.86)	50	—	Olive
K ₂ [Ni (HL ₂) ₂ Cl ₂]2H ₂ O C ₂₆ H ₂₀ N ₄ O ₄ K ₂ Cl ₄ Ni	44.62 (42.69)	2.18 (2.73)	6.00 (7.66)	7.70 (8.03)	70.87	—	Olive
K ₂ [Ni(HL ₃) ₂ Cl ₂] C ₂₈ H ₂₂ N ₄ O ₂ K ₂ Cl ₂ Ni	49.64 (51.4)	2.97 (3.36)	8.30 (8.56)	9.28 (8.97)	52.76	—	Olive
K ₂ [Ni (HL ₄) ₂ Cl ₂]3H ₂ O C ₂₆ H ₁₈ N ₄ O ₄ K ₂ Cl ₆ Ni	38.45 (38.15)	1.70 (2.44)	5.00 (6.84)	8.76 (7.18)	46	—	Olive
[Ni(HL ₅) ₂] C ₃₀ H ₂₆ N ₄ O ₂ Ni	66.92 (67.58)	4.69 (4.88)	10.19 (10.51)	12.73 (11.01)	40	—	Mustard

angles generated from the optimized structure are discussed. All calculations were performed by the Gaussian 09 program.

3.1 | Geometrical parameters

The optimized geometry of HL₄ is shown in Figure 1 as a representative structure. The various bond lengths and angles generated from the structures of the optimized ligand (HL₄) and the complex (**C4**) using Gaussian 09 software were obtained. They show good resemblance to the X-ray structural investigations of similar ligands and complexes reported,^[3,8,9,23] such as the computed bond lengths for HL₄ ligand, O(1)-C(6), O(1)-H(26), N(3)-C(7), N(3)-C(9), N(8)-C(7) and N(8)-C(2) are 1.341, 0.991, 1.378, 1.381, 1.323 and 1.379 Å, respectively. The computed bond angles, C(6)-O(1)-H(26), C(7)-N(3)-C(9), C(7)-N(8)-C(2) and N(8)-C(7)-N(3) in the HL₄ ligand are 108.754, 107.703, 106.468 and 111.237°, respectively. Bond lengths and angles of complexes **C1–C5** were compared with similar compounds in the literature,^[3,8,9,24,25] as

**FIGURE 1** Optimized structure of HL₄ ligand at B3LYP/TZVP level of theory

given in Table 2. The optimized structure of **C4** is shown in Figure 2.

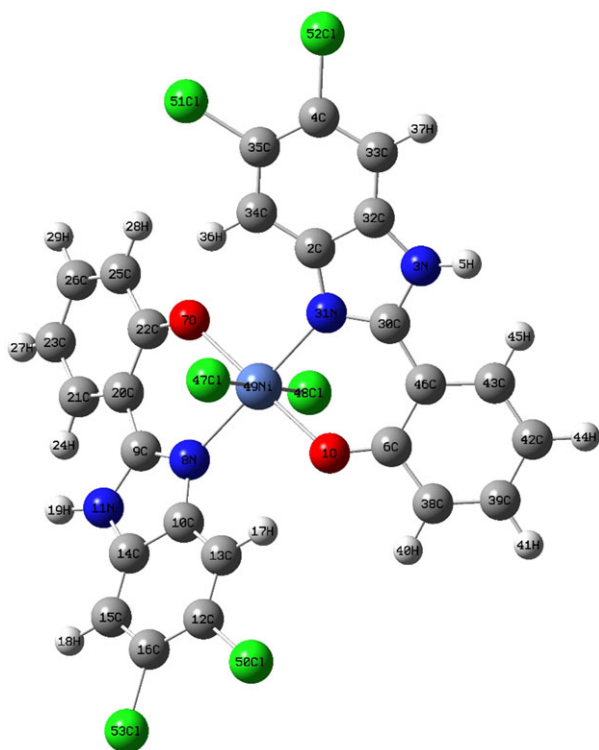
3.2 | FT-IR spectra

To understand the vibrational properties and structural characteristics of the ligands and complexes, the DFT calculations with B3LYP/TZVP level have been used, and the observed bands are assigned based on the results of normal.

The prominent bands in the IR spectra of the ligands and their complexes are presented in Table 3. The measured and calculated FT-IR spectra of the ligand HL₄ and its complex, **C4**, are given in Figures 3a and b, and 4a and b, respectively. In HL₁ spectrum, $\nu(\text{O-H})$ and $\nu(\text{N-H})$ vibration frequencies appear separately at 3325 and 3245 cm⁻¹, respectively, because of weak intramolecular hydrogen bonding.^[26] In HL₂–HL₅ spectra, the characteristic $\nu(\text{O-H})$ and $\nu(\text{N-H})$ vibration frequencies of the ligands exhibit only a single strong band at ~3300 cm⁻¹, probably due to double intramolecular hydrogen bonding between the phenoxyl hydrogen atom and one of the C = N nitrogen atoms. The corresponding peak in the theoretical spectrum was calculated at ~3253 cm⁻¹. The lack of this band in the FT-IR spectra of the complexes indicates coordination through the oxygen atom of the phenolic group to metal. The N–H stretching and bending vibrations of the ligands at ~3200 and ~1490 cm⁻¹ remain either unperturbed or undergo a slight shift in the complexes (~3433 and 1481 cm⁻¹), respectively. The C = C frequencies of phenyl groups in the ligands appeared at ~1591 cm⁻¹ in the IR spectra, and these frequencies are expected to shift at lower frequency upon complex

TABLE 2 Selected bond lengths (Å) and angles (°) for complexes **C1–C5** and similar compounds

	C1	C2	C3	C4	C5	Ref. ^[3]	Ref. ^[8]	Ref. ^[9]	Ref. ^[24]	Ref. ^[25]
Bond lengths										
Ni(49)-O(1)	2.101	2.099	2.105	2.100	1.868	—	—	2.030	—	—
Ni(49)-O(8)	2.101	2.099	2.105	2.099	1.868	—	—	2.031	—	—
Ni(49)-N(9)	2.128	2.122	2.122	2.119	1.927	2.057	2.097	2.056	2.036	2.089
Ni(49)-N(34)	2.128	2.122	2.122	2.119	1.927	—	—	2.056	2.037	—
Ni(49)-Cl(51)	2.536	2.525	2.545	2.519	—	2.388	2.292	—	—	2.264
Ni(49)-Cl(52)	2.530	2.520	2.528	2.510	—	2.384	2.523	—	—	2.312
Bond angles										
O(1)-Ni(49)-Cl(52)	88.87	88.94	88.68	89.02	—	—	—	—	—	—
N(34)-Ni(49)-O(1)	84.98	85.39	84.91	85.37	90.57	—	—	88.27	—	—
N(34)-Ni(49)-Cl(51)	89.31	89.08	89.07	88.97	—	95.23	—	—	—	94.99
O(8)-Ni(49)-Cl(51)	91.12	91.05	91.32	90.96	—	—	—	—	—	—
N(9)-Ni(49)-O(8)	84.99	85.42	84.92	85.37	90.57	—	—	—	—	—
N(9)-Ni(49)-Cl(52)	90.68	90.92	90.91	91.03	—	89.75	89.15	—	—	101.95
N(9)-Ni(49)-N(34)	178.62	178.16	178.16	177.93	176.25	—	—	—	—	—
Cl(51)-Ni(49)-Cl(52)	179.99	179.99	179.99	179.98	—	174.46	—	—	—	—
O(1)-Ni(49)-O(8)	177.75	177.88	177.36	178.05	174.33	—	—	169.85	—	—

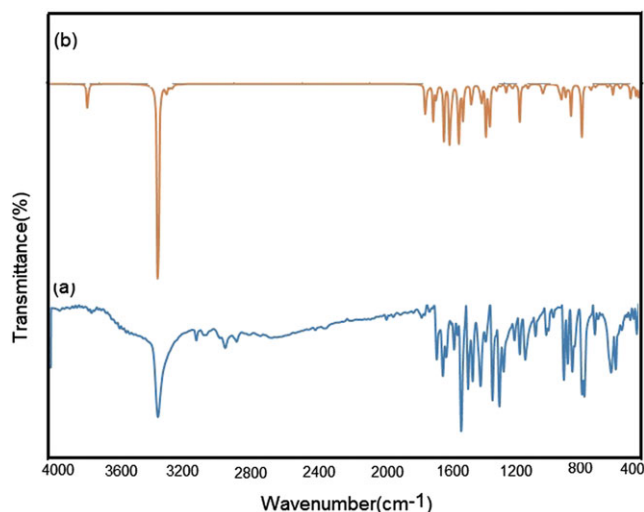
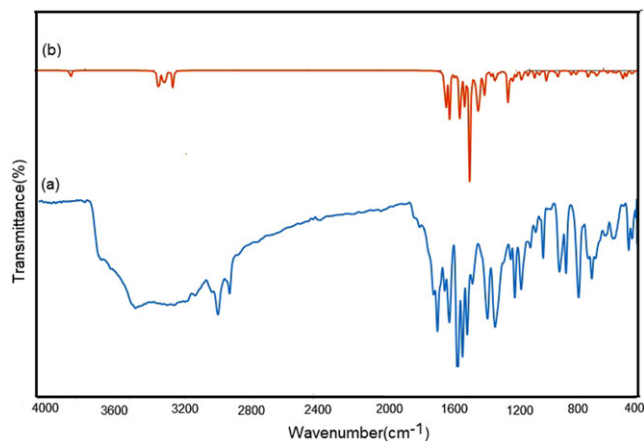
**FIGURE 2** Optimized structure of **C4** complex at B3LYP/TZVP level of theory

formation ($\sim 1562\text{ cm}^{-1}$). The corresponding peaks in predicted theoretical spectra in the ligands and complexes are also calculated at ~ 1560 and $\sim 1552\text{ cm}^{-1}$, respectively. Similarly, the (C = N) asymmetric stretching vibrations

for the ligands are expected to appear at 1637 cm^{-1} . These frequencies are expected to shift at lower frequency upon complex formation (1625 cm^{-1}).^[27] These frequency changes may support the argument that coordination occurs via imine nitrogen atom. The corresponding peaks in the ligands and complexes are also estimated at ~ 1635 and 1633 cm^{-1} in the predicted theoretical spectra. In the IR spectra of the **C1–C5** complexes, the coordination through imine nitrogen atom can also be confirmed by the appearance of a weak band located at the low wave numbers ($\sim 418\text{ cm}^{-1}$) that may be assigned to $\nu(\text{Ni}-\text{N})$.^[28,29] In the high-frequency region, the bands in the range of $3014\text{--}3097\text{ cm}^{-1}$ are attributed to the stretching vibrations of aromatic C-H for all compounds, and the corresponding peaks in the theoretical spectrum are calculated in the range of $3170\text{--}3190\text{ cm}^{-1}$. In **HL₃** and **HL₅**, the bands at $2970\text{--}2858\text{ cm}^{-1}$ are related to the stretching vibrations of aliphatic C-H.^[30] In **HL₂** and **HL₄**, the bands at 1058 and 1097 cm^{-1} correspond to the stretching vibrations of C-Cl, respectively. The sharp or medium bands in the ligands and their complexes in the range of $675\text{--}864\text{ cm}^{-1}$ are due to the out-of-plane deformation bands for the aromatic C-H.^[26] In the spectra of free ligands, there is a band at about 1298 cm^{-1} , which is assigned to $\nu(\text{C}-\text{O})$ of the phenolic group. The phenolic C-O band of the uncoordinated ligand shifts to lower frequencies during complex formation. The phenolic C-O band at about $\sim 1261\text{ cm}^{-1}$ in spectra of the presented complexes suggests that the phenolic oxygen atoms coordinated to the metal.^[31]

TABLE 3 FT-IR spectra data of the compounds under study

Compound	Wavenumber(cm^{-1}), KBr pellets
HL ₁	3325, 3245, 3053, 2300, 1629, 1591, 1490, 1460, 1417, 1394, 1276, 1130, 838, 675
C1	3419, 3058, 2925, 2854, 1623, 1600, 1527, 1481, 1438, 1309, 1255, 1137, 856, 742, 486, 418
HL ₂	3328, 3014, 2310, 1633, 1583, 1488, 1465, 1421, 1382, 1282, 1134, 1058, 844, 705
C2	3433, 3176, 3060, 2858, 1623, 1560, 1481, 1452, 1305, 1253, 1137, 929, 705, 511, 480, 418
HL ₃	3236, 3082, 3028, 2914, 2858, 2212, 1735, 1637, 1596, 1488, 1456, 1419, 1390, 1261, 1130, 846, 680
C3	3417, 3180, 3058, 2858, 1628, 1604, 1562, 1481, 1448, 1307, 1261, 1137, 865, 752, 487, 439
HL ₄	3332, 3097, 2320, 1637, 1598, 1487, 1444, 1419, 1371, 1298, 1132, 1097, 864, 740
C4	3419, 3060, 2921, 2852, 1625, 1558, 1481, 1450, 1301, 1255, 1135, 966, 752, 451, 439
HL ₅	3257, 3124, 3049, 2970, 2858, 2241, 1637, 1589, 1488, 1461, 1417, 1384, 1257, 1130, 852, 675
C5	3404, 3055, 2972, 2860, 1635, 1550, 1475, 1442, 1317, 1247, 1134, 840, 746, 476, 430

FIGURE 3 The comparison of (a) experimental FT-IR, (b) theoretical IR, calculated at B3LYP/TZVP level, spectra for ligand HL₄FIGURE 4 The comparison of (a) experimental FT-IR, (b) theoretical IR, calculated at B3LYP/TZVP level, spectra for complex C₄

Overall, in the C₁–C₅ complexes, deprotonation and subsequent involvement of the phenoxyl group in metal coordination could also be supported by the appearance of a new band at a lower frequency (487 cm^{-1}) region assignable to $\nu(\text{Ni-O})$. These results are in agreement with the theoretical calculations. The experimental and calculated IR spectra of ligands and their complexes agree extremely well with respect to their peak frequencies, band intensities and the shapes of the bands.^[32]

3.3 | Electronic spectra

The UV–Vis spectra data of HL_{1–5} ligands and C₁, C₂, C₃, C₄ and C₅ complexes are given in Table 4. The UV–Vis spectra in DMSO solvent were measured from 200 to 800 nm. The observed bands at lower wavelength (210–300 nm) correspond to $\pi \rightarrow \pi^*$ transitions of the aromatic rings. The bands in the range of 310–360 nm are due to $n \rightarrow \pi^*$ transitions.^[31] The electronic spectra of the C₁, C₂, C₄ and C₅ complexes are of little help in the present case, as the $d \rightarrow d$ transitions are masked by the strong charge-transfer bands.^[33] In the electronic spectra

TABLE 4 UV-vis spectra data of the compounds (DMSO as solvent)

Compound	UV (nm)	Vis.
HL ₁	250, 290	320
HL ₂	220, 240, 270, 290	310, 330
HL ₃	210, 240, 300	320, 340
HL ₄	300	340, 360
HL ₅	210, 240, 290	340
C1	—	350
C2	—	390
C3	—	360, 390
C4	—	390
C5	—	370

of the **C1**, **C2**, **C4** and **C5** complexes, there are broad bands at 350, 390 and 370 nm, respectively, because of the combination of chloride \rightarrow metal or oxygen \rightarrow metal, nitrogen \rightarrow metal charge transfers (L \rightarrow Ni charge transfer). The electronic spectrum of the **C3** complex shows the two weak bands. The bands in the visible region (360 and 390 nm) may be assigned to $^3A_2g(F) \rightarrow ^3T_{1g}(P)$ and $^3A_2g(F) \rightarrow ^3T_{1g}(F)$ transitions, respectively. The $^3A_2g(F) \rightarrow ^3T_{2g}(F)$ transition is not observed in the spectrum of the present complex; it is seldom observed as it is inherently weak due to an orbital selection rule.^[34] These are characteristic for high spin octahedral geometry for the **C3** complex.

3.4 | NMR spectra of ligands

1H -NMR spectra data of the ligands and the assignments of the peaks were given in Table 5. The 1H -NMR spectra of HL₃, HL₄ and HL₅ ligands exhibit only a singlet broad peak for the OH and amine NH protons (13.14, 12.5 and 13.11 ppm for HL₃, HL₄ and HL₅, respectively). This broadening results from strong intramolecular hydrogen bonding between the amine nitrogen atom with double bond and phenolic hydrogen atoms. The HL₁ and HL₂ ligands give two singlet peaks for OH and NH protons (13.07 and 9.44 ppm for HL₁, 13.26 and 12.76 ppm for HL₂, respectively).^[35] In HL₁₋₅ ligands, protons of the phenolic ring moiety appeared at the same position but with different chemical shifts. This is due to the substitutions on the ring that have affected the phenolic ring moiety. For example, proton chemical shifts of HL₂ and HL₄ (containing electron-withdrawing groups of Cl), appear at higher ppm than HL₁ (non-substituted), HL₃ and HL₅ (containing electron-donating groups of CH₃). In the 1H -NMR spectra of HL₃ (included a methyl group) and HL₅ (included two methyl groups), there are singlets at 2.42 and 2.32 ppm, respectively. The position of protons and the assignments of the peaks in the benzimidazole moiety in HL₁₋₅ ligands is different (Table 5). Also, 1H -NMR spectra of the ligands are shown in Figure S1.

In the ^{13}C -NMR spectra of the HL₁₋₅ ligands, the signals at about 157.71–158.98 ppm and 150.83–153.77 ppm are attributed to carbon atoms bonded to the OH oxygen atom and carbon atom of imidazole group, respectively.^[26] The other signals are related to the benzimidazole and phenolic ring carbon atoms (Table 6).

3.5 | Theoretical calculation and stability

According to the DFT calculations, HL₄, HL₂ and their Ni(II) complexes, **C4** and **C2**, have lower energy values

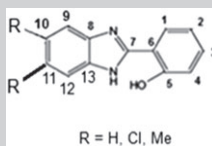
TABLE 5 1H -NMR spectra data: The chemical shift values (δ_{HI} , ppm) with coupling constants (J , Hz)

Ligands	Benzimidazole protons			Phenolic protons						
	H ₁	H ₂	H ₂ '	NH	CH ₃	H ₃	H ₄	H ₃ '	H ₅	OH
HL ₁	7.72 s	7.58 d J = 12.72	—	9.44 s	—	7.14 d J = 8.30	6.96 t J = 7.35	7.32 m	7.32 m	13.07 s
HL ₂	7.64 s	7.74 d	7.26 d J = 8.37	12.76 s	—	8.04 d J = 7.7	7.37 t J = 7.59	7.01 m	7.01 m	13.26 s
HL ₃	7.43 s	7.53 d J = 8.13	7.08 d J = 8.16	13.14 s	2.42 s	8.03 d J = 7.71	7.35 t J = 7.26	7.01 m	7.01 m	13.14 s
HL ₄	7.87 s	—	7.87 s	12.50 s, br	—	8.05 d J = 7.66	7.38 t J = 7.48	7.01 m	7.01 m	12.05 s, br
HL ₅	7.40 s	—	7.40 s	13.11 s	2.32 s	8.00 d J = 7.69	7.33 t J = 7.56	6.98 m	6.98 m	13.11 s

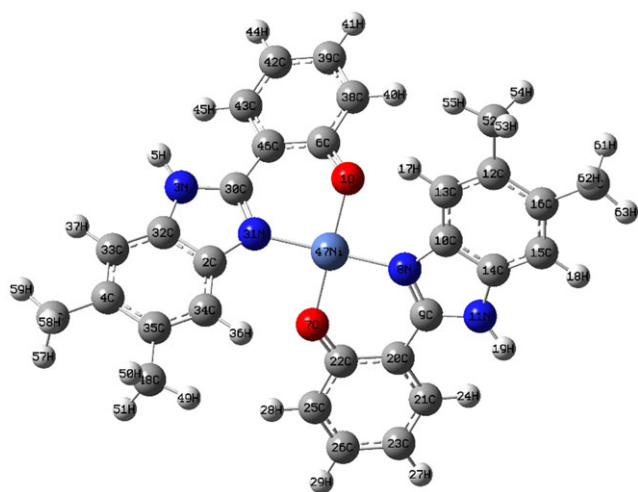
m, multiplet; s, singlet; br, broad; d, doublet; t, triplet.

TABLE 6 ^{13}C -NMR spectral data of the HL_{1-5} (δ_{C} , ppm; in DMSO-d_6)

Ligands	Chemical shifts (δ_{C} , ppm)
HL₁	112.08, 118.16, 119.02, 123.34, 124.37, 132.04, 151.35, 158.98
HL₂	112.52, 117.23, 117.50, 117.65, 119.27, 123.07, 126.59, 132.05, 152.85, 157.87
HL₃	21.29, 112.69, 117.15, 119.05, 124.29, 126.05, 131.54, 132.26, 151.40, 157.98
HL₄	112.54, 116.08, 117.21, 119.36, 124.99, 127.00, 132.30, 133.53, 153.77, 157.71
HL₅	19.96, 112.79, 117.08, 118.96, 125.88, 131.31, 131.48, 150.83, 157.92



of -1606 , -1146 , -5639 , -4720 a.u., respectively. The total energy values of HL_1 , HL_3 , HL_5 and their complexes **C1**, **C3** and **C5** are: -686 , -726 , -765 , -3801 , -3879 and -3037 a.u., respectively. The DFT calculations prove that the chloro derivatives have higher stability than the methyl derivatives, comparing them with each other. It is observed that HL_4 , having two chloro substituents, is more stable (total energy: -1606 a.u.) than HL_2 , having one chloro substituent (-1146 a.u.). The DFT calculations show that the stability of the HL_1 ligand is the lowest among the ligands. Likewise, **C5** has the highest energy among the complexes and consequently the lowest stability, -3037 a.u., because of the absence of chloro atoms attached to Ni (Figure 5). According to the geometry optimization of **C1–C4** structures with DFT calculations, Ni was located on an octahedral center with the C = N nitrogen and hydroxy oxygen atoms of benzimidazole moiety and phenol ring, respectively, associated with two chloride ions. But for the **C5** complex, there is a square-planar geometry with Ni ion in the center that coordinated to the

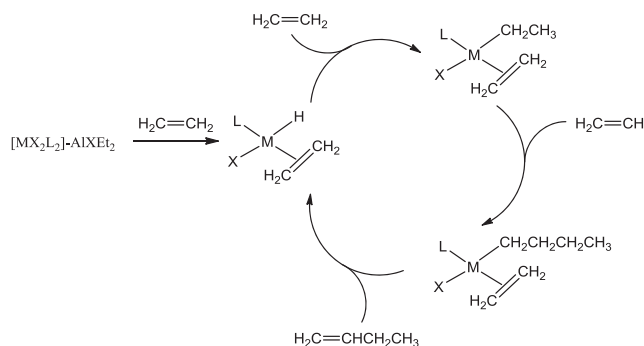
**FIGURE 5** Optimized structure of **C5** complex at B3LYP/TZVP level of theory

C = N nitrogen and hydroxy oxygen atoms (molecular symmetry: D_2h for **C1–C5** complexes).

3.6 | Ethylene oligomerization

The catalytic activities of all pre-catalysts for ethylene oligomerization have been carried out in the presence of Et_2AlCl as co-catalyst. In all cases, these catalysts generate butenes and hexenes as the main oligomeric products, and the distribution of oligomers does not follow Schulz–Flory rules. No odd carbon number oligomers were detected in the GC analysis.^[36]

In the oligomerization mechanism of this class of catalysts, at first, active species are formed through interaction of nickel complex with co-catalyst (such as Et_2AlCl and MAO) under an ethylene atmosphere. The catalytically active species is probably a square-planar or octahedral hybridized nickel atom interacting with a hydride (or alkyl), electronegative groups (x), the ligand donor atoms and ethylene molecule. Then, by using successive insertion of ethylene, an intermediate species alkyl-nickel during the growth step of chains is formed. After that, by β -hydrogen elimination, hydride species and oligomer chains are released (Figure 6).^[37] Overall, the nickel hydride species can be generated by a variety of

**FIGURE 6** Reaction mechanism for ethylene oligomerization by nickel (II) catalyst

standard organometallic reactions, including β -hydride transfer from an intermediate nickel alkyl and oxidative addition of a Lewis acid to a zero-valent nickel species. The labile cationic nickel species containing vacant sites should be stabilized by the coordination of an ethylene molecule. The reaction mechanism for ethylene oligomerization with nickel (II) catalysts was given in Figure 6.

3.6.1 | Ethylene oligomerization by nickel complexes C1–C5

The nickel (II) complexes, **C1–C5**, were systematically investigated for the oligomerization of ethylene by using AlEt_2Cl as co-catalyst. In the **C1** complex, dimerization, trimerization and tetramerization of ethylene are the major reactions, and the selectivity of 1-octeneproductin total is high according to GC analysis, while **C4** and **C5** complexes showed both dimer and trimer products with good selectivity modest to high toward 1-butene and 1-hexene. Also, **C2** and **C3** displayed good selectivity of 1-buten with a dimer as the predominate product. The results of ethylene oligomerization were collected in Table 7.

According to Table 7 (entries 1–5), the oligomerization activities decreased in the order of **C2** > **C3** > **C4** > **C5** > **C1**. From this comparison, we can see that **C1** and **C2** complexes showed the lowest and highest catalytic activities, respectively. The R substituents had

different influences on the catalytic performances. When the nickel complex contains halide as the electron-withdrawing substituent on the aryl ring (**C2**), the reactivity is much higher than with alkyl substituent. The electron-withdrawing group on the benzimidazol rings makes the central metal more positive and leads to a decrease of the electron density in the benzimidazol rings, so the ethylene can easily coordinate to nickel species, which finally led to higher catalytic activity.^[3] This complex showed high selectivity for 1-butene. In general, electron-withdrawing substituents enhance catalyst activities, as do less bulky substituents, but when the number of Cl atoms in the ligand (**C4**) increases, catalytic activity decreases. This phenomenon is caused by the low solubility of complex. The complexes with ligands that have methyl substituents (**C3**) enhance their solubility and stability of active species due to less exposure to impurity reactants,^[38] and for these catalysts only dimerization was achieved, with a high selectivity for 1-butene. Whereas, the **C5** complex contains two methyl groups on the benzimidazol rings that might push more electrons to the nickel atom, reduce the net charge on the nickel center and, therefore, result in lower catalytic activity. In general, increasing steric hindrance leads to a decrease in the catalytic activities resulting in a lower positive charge on nickel of the active catalytic species, which, subsequently, weakens the metal–ethylene interaction during the ethylene oligomerization.^[36] Also, a possible

TABLE 7 Results of ethylene oligomerization with **C1–C5**^a and its comparison with similar complexes^{d–h}

Entry	Precatalyst	Temperature (°C)	Al/Ni	Time (min)	Pressure (atm)	Yield (g)	Activity ^b	Oligomer distribution ^c (%)					
								C ₄	C ₆	C ₈	α -C ₄	α -C ₆	α -C ₈
1	C1	30	200	30	20	1.84	368	86.60	12.63	0.77	89.04	57.14	100
2	C2	30	200	30	20	33.00	6600	100	—	—	100	—	—
3	C3	30	200	30	20	11.42	2284	100	—	—	92.31	—	—
4	C4	30	200	30	20	9.20	1840	66.67	33.33	—	100	100	—
5	C5	30	200	30	20	8.59	1718	97.74	2.26	—	83.89	100	—
6 ^d	Ref. ^[3]	20	1000	30	20	—	2240	93.8	6.2	—	—	—	—
7 ^e	Ref. ^[8]	30	700	10	10	—	5200	99.8	0.2	—	—	—	—
8 ^f	Ref. ^[9]	20	200	30	1	—	301	92.4	7.6	—	—	—	—
9 ^g	Ref. ^[24]	15	1500	30	1	—	235	8.0	18.7	73.3	—	—	—
10 ^h	Ref. ^[25]	30	400	30	10	—	1740	89.7	10.3	—	—	—	—

^aGeneral conditions: 10 μmol of precatalyst, 100 ml toluene as solvent, co-catalyst: Et_2AlCl .

^bIn units of $\text{kg mol}^{-1} \text{h}^{-1}$.

^cDetermined by GC. ΣC denotes the total amounts of oligomers.

^dGeneral conditions: 5 μmol of precatalyst, toluene (100 ml), co-catalyst: Et_2AlCl .

^eGeneral conditions: 5 μmol of precatalyst, toluene (100 ml), co-catalyst: Et_2AlCl .

^fGeneral conditions: 5 μmol of precatalyst, toluene (30 ml), co-catalyst: Et_2AlCl .

^gGeneral conditions: 5 μmol of precatalyst, toluene (100 ml), co-catalyst: MAO.

^hGeneral conditions: 5 μmol of precatalyst, toluene (100 ml), co-catalyst: Et_2AlCl .

explanation is that in late transition-metal catalytic systems, both bulkier and more electron-rich ligands weaken the interactions between the metal center and the incoming monomer, and thereby retard the rate of ethylene insertion. The observed activity trends appear to be a superposition of electronic and steric factors.^[39]

In addition, we compared the catalytic performance of **C1–C5** with similar complexes in the literature (Table 7).^[3,8,9,24,25] As can be seen, **C1–C5** complexes could be easily activated with a lower amount of co-catalyst (Et_2AlCl) ($\text{Al/Co} = 200$), and exhibited higher activities as well as better selectivity toward 1-butene and 1-hexene formation in ethylene oligomerization.

Furthermore, in the present work, neither wax nor polymer were formed in the oligomerization using synthesized catalysts; however, in most of the published works, in addition to oligomer, a low amount of polymer has been formed as well. This indicates that our synthesized catalysts are suitable for oligomer production.

4 | CONCLUSIONS

In summary, we report the synthesis and characterization of 2-(1H-benzimidazol-2-yl)-phenol derivatives and their Ni(II) complexes. In conclusion, the structures of the mononuclear complexes were verified by FT-IR, UV-Vis and ICP, as well as by elemental analysis (C, H and N). All the analytical and spectral data are consistent with theoretical calculations. According to the geometry optimizations obtained from DFT calculations, Ni(II) ion in the complexes is located on an octahedral and/or square-planar center. The catalytic activities and distribution of oligomers were significantly affected by the environment of the ligands. Nickel complexes could be easily activated in the presence of Et_2AlCl , and exhibited much higher activities for ethylene oligomerization, even though the amount of co-catalyst was very small and the main products were dimers and trimers of ethylene and increased the selectivity for α -olefins.

ACKNOWLEDGEMENTS

This work was supported by Iran University of Science and Technology, Iran Polymer and Petrochemical Institute and Petrochemical Research & Technology Company. Naeimeh Bahri-Laleh thanks MOLNAC (www.molnac.unisa.it) for its computer facilities.

ORCID

Azadeh Tadjarodi  <http://orcid.org/0000-0003-0496-2322>

REFERENCES

- [1] W. H. Sun, S. Jie, S. Zhang, W. Zhang, Y. Song, H. Ma, *Organometallics* **2006**, *25*, 666.
- [2] P. Hao, S. Zhang, W. H. Sun, Q. Shi, S. Adewuyi, X. Lu, P. Li, *Organometallics* **2007**, *26*, 2439.
- [3] B. Y. Su, J. S. Zhao, *Polyhedron* **2006**, *25*, 3289.
- [4] S. Jie, S. Zhang, W. H. Sun, *Eur. J. Inorg. Chem.* **2007**, *35*, 5584.
- [5] O. Dayan, M. Tercan, N. Ozdemir, *J. Mol. Struct.* **2016**, *1123*, 35.
- [6] A. SelcenAlpan, Ö. Yılmaz, O. Kılıçkaya, P. Kara, H. SemihGüneş, M. ŞengünÖzsöz, *J. Marmara Pharm.* **2012**, *16*, 48.
- [7] D. T. Nannapaneni, Atyam VSSS Gupta, M. I. Reddy, Raidu Ch Sarva, *J. Young Pharm.* **2010**, *2*, 273.
- [8] X. Chen, L. Zhang, T. Liang, X. Hao, W. H. Sun, *C. R. Chimie.* **2010**, *13*, 1450.
- [9] Q. Shi, S. Zhang, F. Chang, P. Hao, W. H. Sun, *J. C. R. Chimie* **2007**, *10*, 1200.
- [10] C. Lee, W. Yang, R. G. Parr, *J. Phys. Res. Part B* **1988**, *37*, 785.
- [11] A. D. Becke, *J. Chem. Phys.* **1993**, *98*, 1372.
- [12] F. Nouri Ahangarani, N. Bahri-Laleh, M. NekoomaneshHaghighi, *Des. Monomers Polym.* **2016**, *19*, 394.
- [13] N. Bahri-Laleh, A. Poater, L. Cavallo, S. A. Mirmohammadi, *Dalton. Trans.* **2014**, 43.
- [14] A. Correa, N. Bahri-Laleh, L. Cavallo, *Macromo. Chem. Phys.* **2013**, *214*, 1980.
- [15] N. Bahri-Laleh, L. Falivene, L. Cavallo, *Polyolefin. J.* **2014**, *1*, 139.
- [16] A. Poater, L. Falivene, C. A. Urbina Blanco, S. Manzini, S. P. Nolan, L. Cavallo, *Dalton. Trans.* **2013**, *42*, 7433.
- [17] A. Schäfer, H. Horn, R. Ahlrichs, *J. Chem. Phys.* **1992**, *97*, 2571.
- [18] M. J. Frisch, G. W. Trucks, H. B. Schlegel, *Gaussian 09*, Gaussian, Inc., Wallingford CT **2009**.
- [19] S. Kundu, S. Biswas, A. Sau Mondal, P. Roy, T. Kumar Mondal, *J. Mol. Struct.* **2015**, *1100*, 27.
- [20] M. M. Ibrahim, A. M. M. Ramadan, H. S. El Sheshtawy, M. A. Mohamed, M. Soliman, S. Imam, *J. Coord. Chem.* **2015**, *68*, 4296.
- [21] R. C. Mauryaa, B. A. Malika, J. M. Mira, P. K. Vishwakarmaa, D. K. Rajaka, N. Jaina, *J. Coord. Chem.* **2015**, *68*, 2902.
- [22] A. Tavman, S. Ikiz, A. FundaBagcigil, N. Yakutözgür, S. Ak, *J. Serb. Chem. Soc.* **2009**, *74*, 537.
- [23] L. L. Han, *J. ActaCryst. E* **2010**, *66*, o2047.
- [24] J. Du, L. J. Li, Y. Li, *J. Inorg. Chem. Commun.* **2005**, *8*, 246.
- [25] Y. Chen, P. Hao, W. Zuo, K. Gao, W. H. Sun, *J. Organomet. Chem.* **2008**, *693*, 1829.
- [26] A. Tavman, I. Boz, A. SeherBirteksöz, *J. Spectrochim. Acta Part A* **2010**, *77*, 199.
- [27] P. P. Hankare, L. V. Gavali, V. M. Bhuse, S. D. Delekar, R. S. Rokade, *Indian J. Chem.* **2004**, *43A*, 2578.
- [28] S. S. Qian, X. L. Zhao, L. H. Pang, Z. L. You, H. L. Zhu, *J. Coord. Chem.* **2016**, *42*, 345.
- [29] M. M. Abdelzaher, *J. Appl. Organomet. Chem.* **2004**, *18*, 149.

- [30] H. İlkimen, C. Yenikaya, A. Gülbandılar, M. Sarı, *J. Mol. Struct.* **2016**, 1120, 25.
- [31] A. Tavman, I. Boz, A. SeherBirteksöz, A. Cinarlı, *J. Coord. Chem.* **2010**, 63, 1398.
- [32] P. Saha, J. Prakash Naskar, A. Bhattacharya, R. Ganguly, B. Saha, S. Chowdhury, *J. Coord. Chem.* **2016**, 69, 303.
- [33] A. Tavman, *J. Transit. Metal. Chem.* **2006**, 31, 194.
- [34] K. K. Mohammed Yusuff, R. Sreekala, *J. Thermochim. Acta* **1991**, 179, 313.
- [35] A. Tavman, S. İkiz, A. FundaBagcigil, N. Yakutözgür, S. Ak, *J. Bull. Chem. Soc. Ethiop.* **2010**, 24, 391.
- [36] X. Tang, W. H. Sun, T. Gao, J. Hou, J. Chen, W. Chen, *J. Organomet. Chem.* **2005**, 690, 1570.
- [37] I. Kim, C. Hun Kwak, J. Sung Kim, C. S. Ha, *J. Appl. Catal. A Gen.* **2005**, 287, 98.
- [38] S. Song, R. Gao, M. Zhang, Y. Li, F. Wang, W. H. Sun, *J. Inorg. Chim. Acta.* **2011**, 376, 373.
- [39] R. Gao, K. Wang, Y. Li, F. Wang, W. H. Sun, C. Redshaw, M. Bochmann, *J. Mol. Catal. A: Chem.* **2009**, 309, 166.

SUPPORTING INFORMATION

Additional Supporting Information may be found online in the supporting information tab for this article.

How to cite this article: Haghverdi M, Tadjarodi A, Bahri-Laleh N, Nekoomanesh-Haghighi M. Synthesis and characterization of Ni(II) complexes bearing of 2-(1*H*-benzimidazol-2-yl)-phenol derivatives as highly active catalysts for ethylene oligomerization. *Appl Organometal Chem.* 2017: e4015. <https://doi.org/10.1002/aoc.4015>